

# Experimental evaluation of the performance of earth levees deteriorated by wildlife activities

Gholamreza Saghaee · Ahmad A. Mousa ·  
Mohamed A. Meguid

Received: 24 September 2014 / Accepted: 20 January 2015 / Published online: 17 February 2015  
© Springer-Verlag Berlin Heidelberg 2015

**Abstract** In this study, an earth levee model is constructed to investigate the impact of animal burrows on the integrity and performance of earthen structures. A series of centrifuge experiments are conducted on homogenous scaled-down 1H:1V levee models built from the natural Kasama soil. Both intact and deteriorated models were subject to a 35g acceleration level. Invasive animal intrusions were introduced in the form of horizontal array of idealized cylindrical burrows at the mid-height of the levee. The water level was gradually increased during the centrifuge flight, and the response of the levee was monitored throughout the test. Pore pressures were recorded using pressure transducers placed at preselected locations within the model. Surface displacements were measured using laser LVDTs and supplemented with three digital cameras for tracking the overall deformation pattern of the levee model. A summary of the test procedure and selected results is presented herewith. The observed deformation mechanism due to the presence of animal burrows is also described. As compared with the intact levee, the presence of burrows is found to alter the pattern of the water flow through the deteriorated levee structure—leading to a notable increase in the exit hydraulic gradient, internal erosion, and subsequently slope failure.

**Keywords** Animal burrows · Centrifuge models · Internal erosion · Levee · Seepage

## 1 Introduction

Levee breaches are typically driven by excessive forces from the retained water (floods), weaknesses in the levee material or its foundation, and seismic events. Invasive animal activities have been known to negatively impact the hydraulic performance and often the structural integrity of levees and earth dams. The possible types of deterioration in levees due to wildlife activities can be categorized into structural damage, surface erosion, and hydraulic alterations [10]. The latter, one of the most common causes of failure in earthen structures, can develop in the form of distortion in flow net, internal erosion, and piping [9]. Internal erosion and piping develops in four phases: initiation of erosion, continuation of erosion, forming internal channels, and finally breach [9]. This form of damage may not be visible until the safety of the earth structure is already jeopardized. Internal erosion typically develops when cracks or cavities exist within the earth structure.

The invasive wildlife activities in earthen structures are globally spotted. The estimated worldwide annual cost of damage or failure of earthen structures and the associated infrastructure due to these activities exceeds billions of dollars [2]. Selected case studies of earth structure failures related to wildlife are summarized in Table 1. Although several methods have been used to detect and locate animal cavities in earthen structures, e.g., gravity survey, resistivity methods, seismic reflection, and ground penetrating radar, the damage caused by these nuisance activities could remain concealed for a long time [4].

---

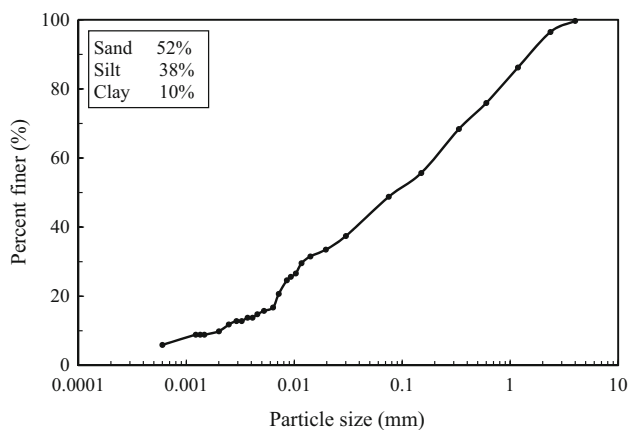
G. Saghaee · M. A. Meguid (✉)  
Department of Civil Engineering and Applied Mechanics,  
McGill University, Montreal, QC H3A 0C3, Canada  
e-mail: mohamed.meguid@mcgill.ca

G. Saghaee  
e-mail: gholamreza.saghaee@mail.mcgill.ca

A. A. Mousa  
School of Engineering, Monash University, Selangor, Malaysia  
e-mail: ahmad.mousa@monash.edu

**Table 1** Reported levee and earth dam failures induced by wildlife invasive activities

Case	Location	Year	Failure mode
Sid White	Near Omak, Washington	1971	Seepage through animal burrows caused dam to fail and dumped debris into town of Riverside [29]
Lower Jones Tract	California Delta	1980	Seepage and rodent activities [11]
Water's Edge	North of Cincinnati, Ohio	1992	Water flow through animal burrows [30]
Iowa Beef Processor Waste Pond	Wallula near Richland, Washington	1993	Uncontrolled seepage through the animal burrows, exiting on the downstream face and causing erosion [20]
Persimon Creek Watershed-Site 50	Mississippi	1998	The dam failed due to erosion of an emergence spillway. Ongoing beaver activities clogged primary spillway [21]
Pischieri Pond	Cleveland, Ohio	1999	The dam was breached when an inspection found a void within its body [30]
Upper Jones Tract	California Delta	2004	High tide, under-seepage and rodent activities [19]
Foenna Stream	Sinalunga, Italy	2006	Porcupine burrow, internal erosion and levee subsidence [7]
Pin Oak	Winfield, Missouri	2008	Muskrat burrows [27]

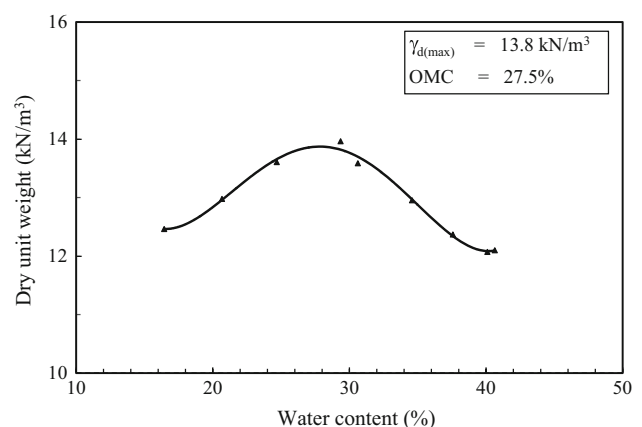
**Fig. 1** Grain size distribution of Kasama soil

Extensive research has been done on intact earth structures to study the mechanisms of piping [3, 24, 28, 31], erosion [5, 6, 18], overtopping [23, 25], and their back analysis [1, 26]. A significant amount of the literature in the area of wildlife investigates the ecological and environmental impact of animal activities and habitat [2]. However, the literature pertinent to the synthesis of failure mechanisms of earth structures due to invasive wildlife activities is very scarce.

This study experimentally investigates the effects of invasive animal activities on the hydraulic performance and stability of levees. Description of the physical model, the methodology used to introduce animal burrows within the model, and details of the performed centrifuge testing are presented. The test results of an instrumented intact (reference) levee model, including surface displacements and pore pressures, are summarized and compared with

**Table 2** Characteristics of Kasama soil

Gravel	0 %
Sand	52 %
Silt	38 %
Clay	10 %
Specific gravity	2.61
Liquid limit	59 %
Plastic limit	33.2 %
Maximum dry density	13.83 kN/m <sup>3</sup>
Optimum moisture content	27.5 %
Friction angle	30°
Cohesion	15 kPa
Hydraulic conductivity	$3.8 \times 10^{-3}$ cm/s

**Fig. 2** Standard proctor test on Kasama soil

those measured for deteriorated levee models. The changes to phreatic surface and the progressive failure developing along the side slopes of deteriorated levees are discussed.

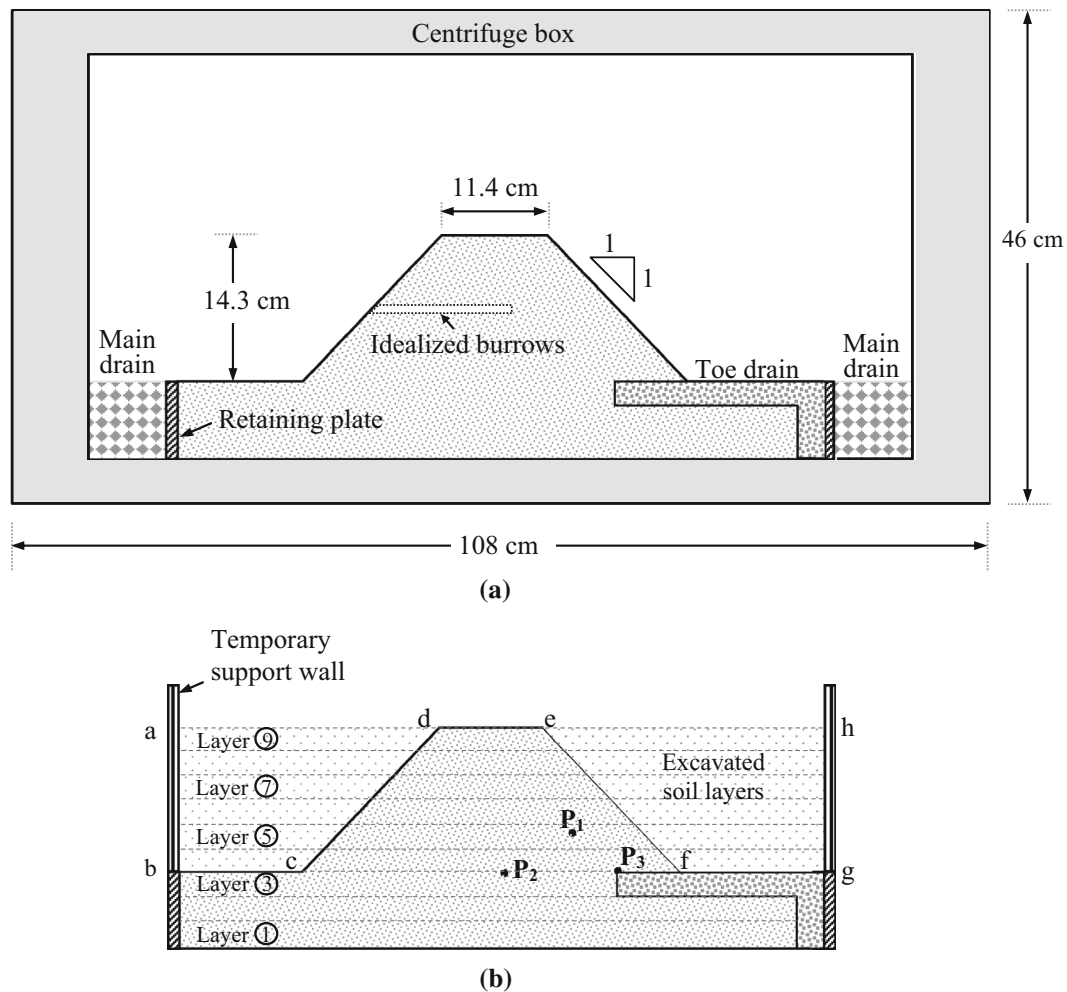


**Fig. 3** Model configurations: **a** geometry; **b** construction procedure and location of pore pressure transducers ( $P_1$  through  $P_3$ )

## 2 Significance and scope of work

The invasive wildlife activities in earth structures have been traditionally dealt with as a maintenance issue rather than a challenging design problem and a long-term performance concern. It is, therefore, instrumental to capture the distinctive hydraulic characteristics as well as the stability of earth structures deteriorated by these intruding activities. The introduction of animal burrows unquestionably alters the original design of earth structures beyond expectations; hence, the challenge in addressing this problem in geotechnical engineering.

Due to the complicated nature of the problems and lack of experimental data needed for validating numerical models, centrifuge testing has been initially chosen for the proposed experimental program on the deteriorated levees. The reported geometry and location of burrows within a levee have been found to vary depending on the water level, animal type, and levee material [2]. Chlaib et al. [8] indicated that animal burrows are mostly found on the

waterside of levees and close to horizontal. For the purpose of this experimental study, animal burrows are idealized as a series of cylindrical openings introduced at the mid-height of the levee along the waterside.

This study aims at identifying the mechanics that govern the progress of failure within the deteriorated levees. Investigation of their hydraulic performance and the impact on stability is closely investigated. Details of the levee model testing are provided in the subsequent section.

## 3 Experimental program

In preparation for an optimized model, a series of simplified two-dimensional limit equilibrium analyses have been performed using SLIDE software [22] with different levee geometries, side slopes, and water levels. The intact levee stability was investigated using Spencer's method for three side slopes: 2.5H: 1V, 1.5H: 1V, and 1H: 1V. Based on the preliminary numerical simulations, an optimized levee

section with equal side slopes and a toe drain are proposed for the purpose of this investigation. The 1H:1V side slope has been found to provide an acceptable balance between stability of the intact levee and a reasonable vulnerability to failure of the deteriorated levee during the proposed testing. Although the chosen geometric configuration may not replicate an existing earth levee, it allows for the development of accelerated failure under the short-term rise in upstream water level. Similar approach was used by other researchers [12, 13] in investigating the failure of embankment dams subjected to seepage conditions.

An array of equally spaced horizontal burrows was then introduced on the waterside at the mid-height of the symmetrical levee. This numerically driven idealizing scheme enabled proper guidance for the design of the physical model used in the study.

The experimental program involves building a scaled-down levee and introduction of idealized animal burrows within the model. Upon completion of the burrow construction, the model was subjected to a gradual increase in water level during centrifuge testing until failure is reached at a predefined gravity acceleration ( $g$ ) level.

Previous studies showed that burrowing animals tend to smartly dig in relatively loose soils that exhibit some cohesion. These favorable geologic conditions ensure efficient excavation while maintaining stability of burrows [14]. The natural Kasama soil, successfully used in similar centrifuge experiments [13], was utilized in this study to mimic these favorable conditions. Kasama soil gradation has been determined based on ASTM D6913 [15] and ASTM D422 [14] (Fig. 1). The soil is classified as silty sand (SM) based on the USCS classification system, with 52 % sand, 38 % silt, and 10 % clay content. A summary of the basic soil properties is given in Table 2. Figure 2 shows the standard proctor results used to determine the maximum dry density of the soil based on ASTM D698 [16].

The geometrical configurations were selected based on the common height of the reported levee failures due to animal burrows [17]. The 1:35 scaled-down section was built to model a 5-m high-levee cross section with a 4-m wide crest width and the selected 1H:1V side slopes. As shown in Fig. 3a, the levee model has a landside toe drain to keep the slope dry and reduce the number of parameters affecting the slope stability of the intact levee. Both intact and deteriorated models were constructed following the same procedure and tested under similar conditions.

### 3.1 Model construction and monitoring scheme

The levee model was constructed inside the centrifuge box using the compaction and excavation technique. This method involves two steps: (1) placement and compaction

of the soil in equal thickness lifts (layers) up to the desired height and (2) removal of the soil (excavation) in order to shape the levee cross section (Fig. 3b). The desired levee profile was overlain on the glass walls of the centrifuge box before soil placement (points  $b$  through  $g$ ). The levee is constructed in nine 2.5-cm thick lifts. Each soil layer is compacted at a moisture content of approximately 30 % using a 57 kN handheld vibratory compactor with plate dimensions of 12 cm in width and 15 cm in length that weighs approximately 57 kN. The toe drain material is placed within the bottom three layers using vertical and horizontal spacers. Upon placing the first two layers (Fig. 3b), the vertical part of the granular toe drain is placed and compacted. The 100 psi (689.5 kPa) miniature pore pressure transducers (PPT) with thin cables (Model GE Druck PDCR 81-347) are placed within the model at preselected locations to monitor the pore pressure changes during the test (Fig. 3b). The use of sufficiently long PPT wires minimizes the impact of wiring interference on the measured deformations. Core samples were collected from both the waterside and landside—away from the levee section—to verify the degree of compaction and the water content before excavation. A total of eight soil samples were extracted from the levee model using a thin-walled

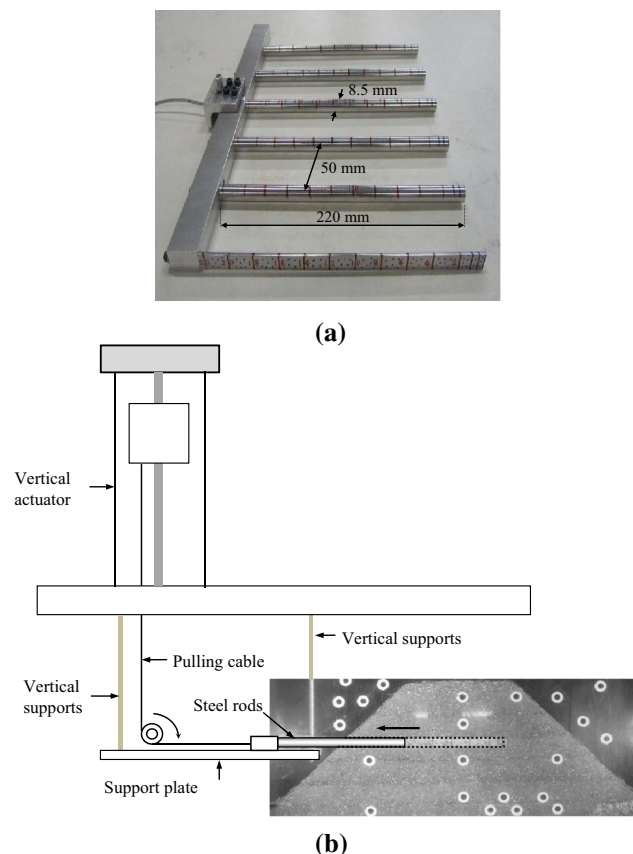


**Fig. 4** Burrow modeling technique: **a** rod set; **b** pullout system

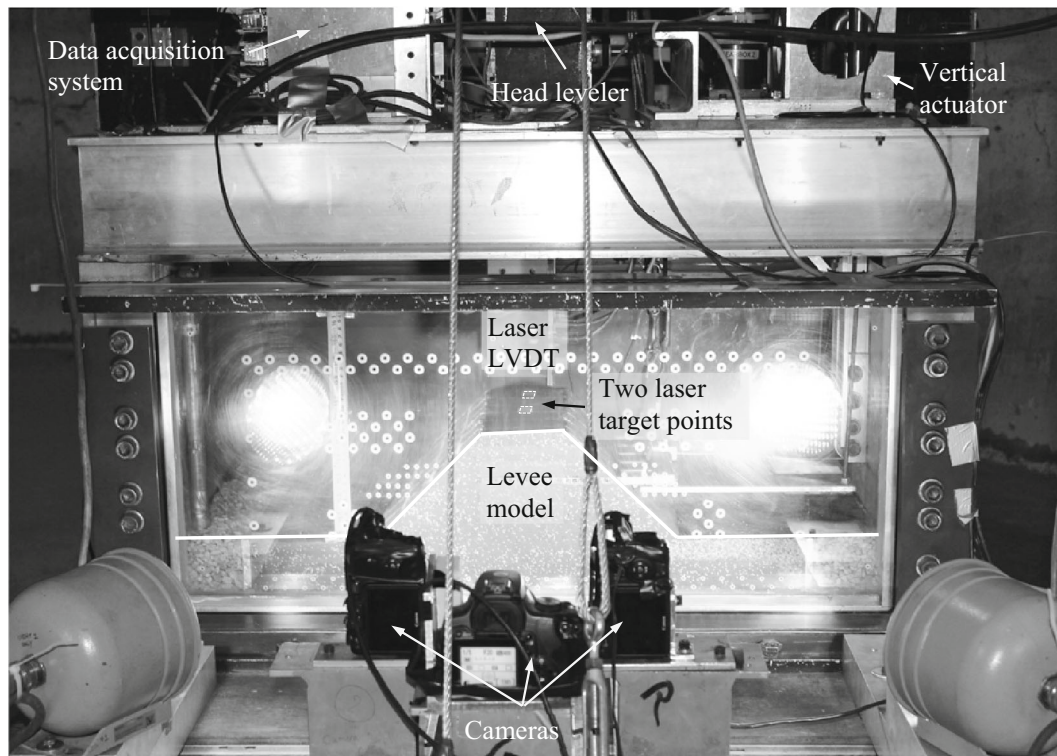


**Fig. 5** Test setup and monitoring system installed on the centrifuge basket

tube sampler of 2.25 cm in diameter. Following the placement of the top layer (layer 9 in Fig. 3b), the excavation process was carried out from the waterside and landside (lines ab and gh) toward the predefined faces (lines cd and ef) of the levee cross section. This necessitated the removal of the soil volume within two trapezoidal areas: abcd and efgh. Excavation is performed slowly in order to minimize disturbance of the levee model. The model profile (points b through g) is continuously monitored during the construction and instrumentation stages. The foregoing scheme was adopted to build both of the intact and deteriorated levee models.

### 3.2 Introduction of idealized burrows into the deteriorated levee model

Burrows were introduced into the built model by initially placing a set of rods, comprised of six 8.5-mm prismatic cylindrical stainless steel rods, at the mid-height of the levee section. The rods are of the same length and spaced 50 mm apart in plan as shown in Fig. 4a. At 35g, the chosen 8.5-mm cavity diameter approximately resembles 300-mm-diameter burrows which is consistent with the size of common wildlife intrusions [2]. The preinstalled rods placed within the model were removed during centrifuge flight using a specially designed pullout system as shown in Fig. 4b. This system consists of a linear actuator, a pulling

cable running over a fixed pulley, and vertical and horizontal support plates (Fig. 4b). The friction along the rod–soil interface was minimized by precise machining and smoothing of the rod surfaces. The rods were marked at preselected equal intervals for tracking of the buried length using a monitoring system installed around the model. Upon reaching the target  $g$ -level (35g), the pullout of the rods array triggered. This technique ensures smooth sliding of the connection beam on the support plate until the rods were completely removed from the model.

Three high-resolution digital cameras (10.0 MP, 6× optical zoom) were placed outside the box to monitor the deformation field of the soil particles during the experiment. Still shots are taken every 5 s throughout the experiment. In addition, the top surface of the model, marked with white paint, is continuously monitored using HD camcorder. Crest settlement has been measured during the tests using two laser LVDTs attached to the box pointing down toward the levee surface. The test setup and monitoring system are illustrated in Fig. 5.

### 3.3 Test procedure

The constructed levee model (14.3 cm height and 11.4 cm width) was tested at a centrifugal acceleration of 35g. The plane-strain box containing the model was equipped with a transparent face to allow for monitoring the deformation of

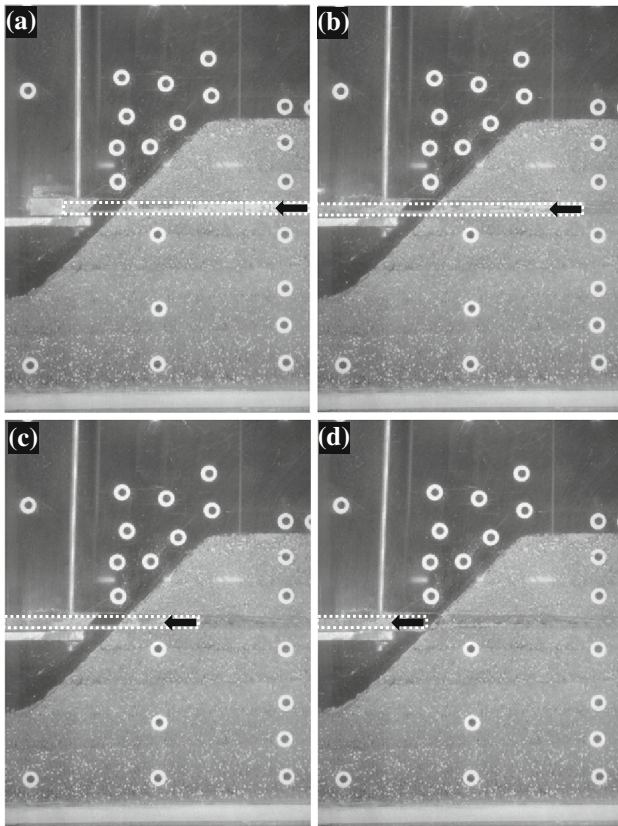


**Fig. 6** Rod set pullout process: **a** initial; **b** half way; **c** three quarters; **d** complete removal

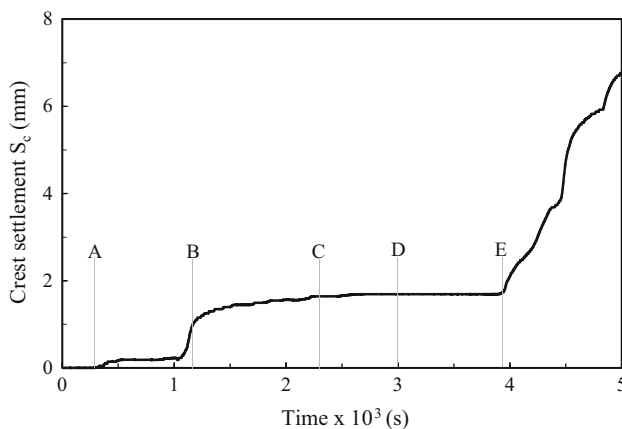


**Fig. 7** Progress of crest settlement during a typical centrifuge flight: **A** spin-up; **B** 35g; **C** beginning of pullout; **D** end of pullout; **E** increase WL

the model. The centrifuge testing started by spinning the model up to an acceleration of 10g. The performance of the model and the installed instruments are checked at this acceleration level to ensure proper monitoring. The centrifuge acceleration continued to increase to the target  $g$ -level (35g), at which the rods were removed. The acceleration is held constant thereafter. Upon rod removal from

the levee body, the water level on the waterside is raised gradually through the waterside main drain located to the left side of the model. A dedicated water pump was used to introduce water from the onboard water tank into the box. The water level is adjusted using the onboard head leveler and monitored using a PPT installed within the main drain.

Figure 6 shows a set of successive images that illustrate the rod removal process as captured by the cameras facing the model. It is crucial to ensure burrow stability before the water level was raised. Therefore, the vertical displacements (settlement) of the levee crest are closely monitored using two laser sensors directed toward the crest during the pullout process. The measured crest settlement versus elapsed time of the centrifuge spin is depicted in Fig. 7. The rods pullout was performed between approximate elapsed times ( $t$ ) of 2,300–3,000 s marked by stages C and D, respectively (Fig. 7). Insignificant settlements were noted during the removal of the rod system. Thus, the cavities introduction and pullout technique seem to provide repeatable initial conditions with a minimal effect on the levee integrity. By inspecting the measured crest settlement of the levee model to up to an elapsed time of 5,000 s, it is evident that the levee started to experience rapid increase in settlement shortly after the water level was raised (at approximate elapsed time of 4,000 s as depicted in Fig. 7).

All centrifuge tests reported in this study have been conducted at the C-Core centrifuge facility in Saint John's, Newfoundland, Canada. The facility has a 5.5-m beam centrifuge with a maximum  $g$ -level of 200  $g$  and 2,200 kg payload capacity at 100  $g$ .

## 4 Results and discussion

### 4.1 Levee deformation

The crest settlement of the intact and deteriorated levee models are shown in Fig. 8. Crest settlement and levee

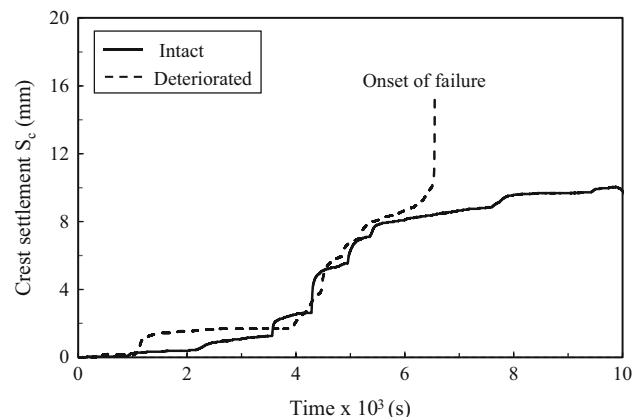


**Fig. 8** Crest settlement of intact and deteriorated levees

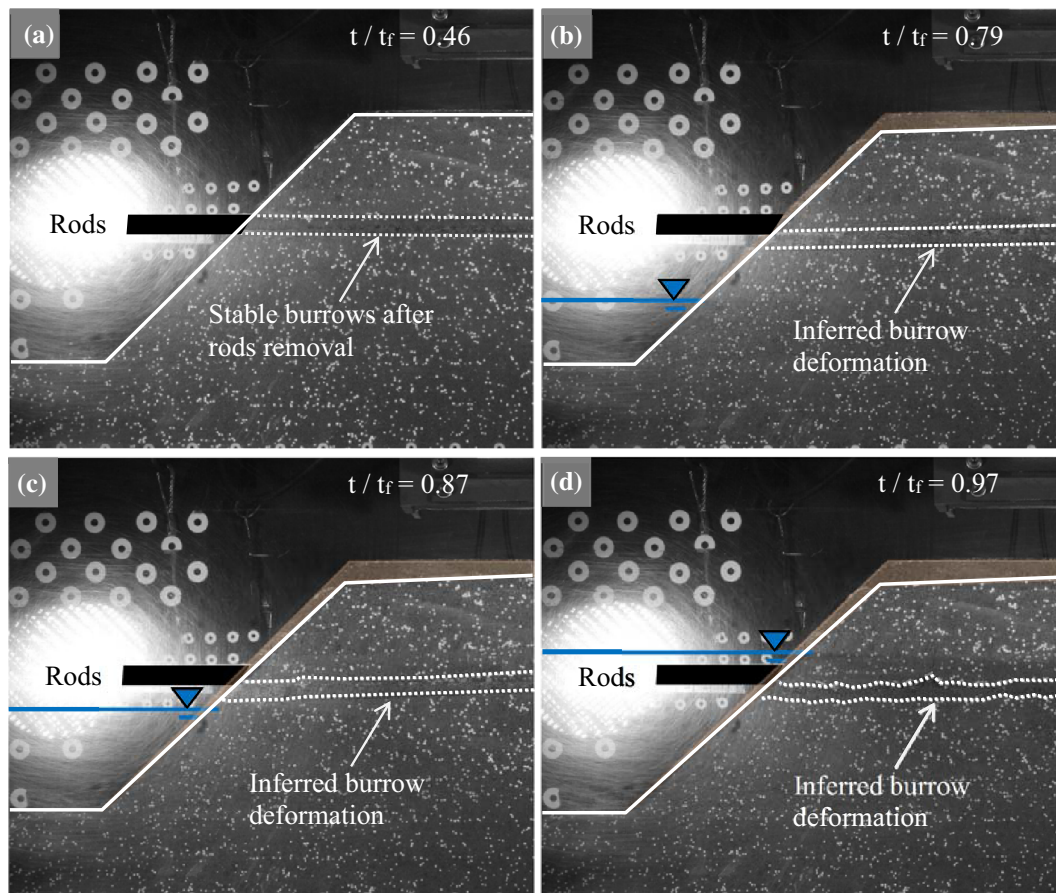


**Fig. 9** Observed crest settlement and traced deformation of burrows: **a** immediately after rod removal; **b** water flow reaches burrows level; **c** upstream water filled the burrows; **d** water level higher than burrows elevation

distortion were closely monitored during testing. For both configurations, the crest experienced a small increase in settlement of about 2 mm prior to the commencement of water ( $t \cong 4,000$  s). The rate of settlement rapidly increased in both cases to about 8 mm shortly afterward ( $t \cong 6,000$  s). This is attributed to the water flow through the levee and the associated increase in pore pressure within the body of the levee and its foundation. Beyond that point, the two configurations exhibit quite distinguishing responses. The crest settlement of the intact levee (indicated by the solid line) stabilizes at about 9 mm, whereas the deteriorated levee (the broken line) experienced excessive settlement (the near vertical line) followed by a rapid failure.

Selected snapshots of the levee cross section were taken at different elapsed times to examine the progression of geometrical changes to the original profile and the burrows following the increase in water level (Fig. 9). The time elapsed is normalized with respect to the levee failure time ( $t_f$ ). The rod location is indicated in dark color to allow for tracking the movement of the burrows during levee settlement. Figure 9a depicts the changes in the levee cross

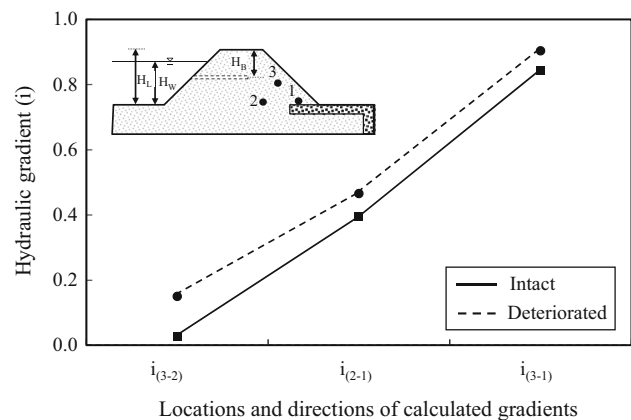


**Fig. 10** Estimated hydraulic gradients near the exit locations

section following the rod set removal and right before elevating the water level. Evidently, the levee geometry is essentially unchanged, and the traced burrow geometry remains in line with the rod set location. When the water level reached about 25 % of the levee height (at  $t/t_f \cong 0.79$ ), downward movement of both the crest and the

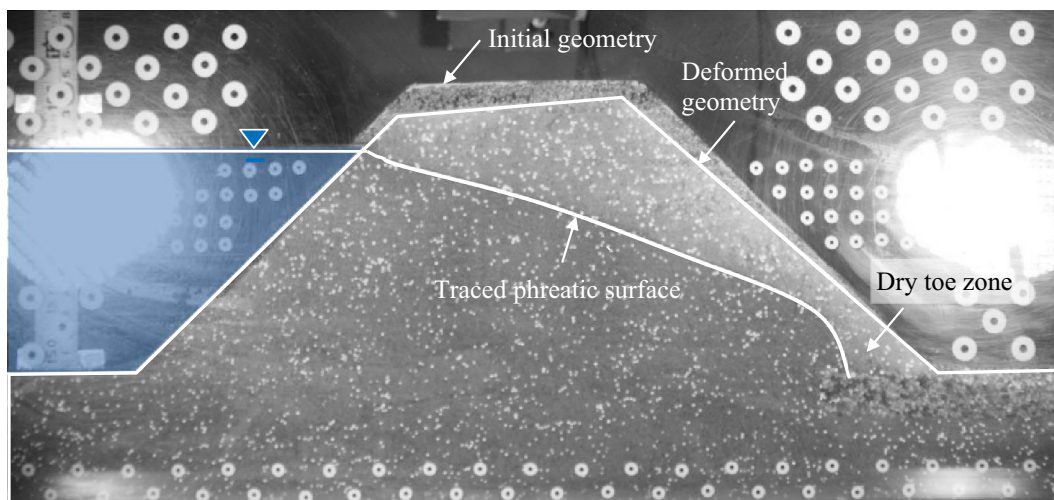


Fig. 11 Observed seepage through the intact levee structure and the inferred phreatic surface

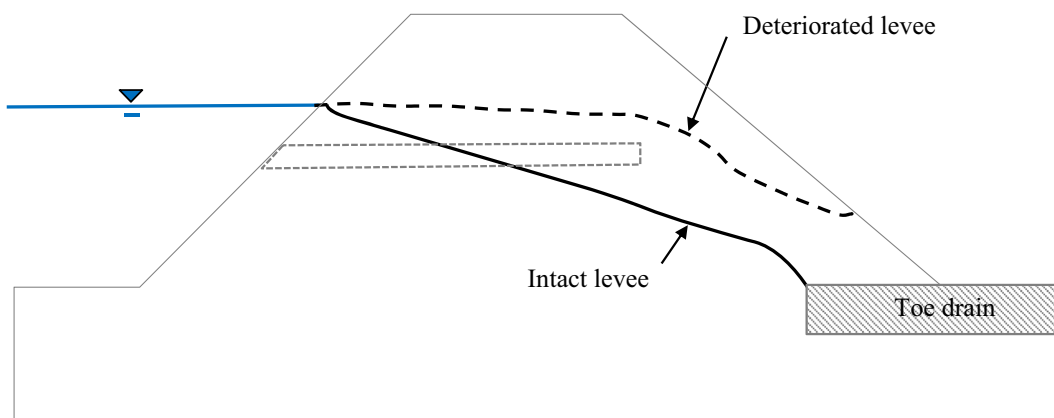


Fig. 12 Conceptual comparison between traced phreatic surfaces for intact and deteriorated levees

burrows is observed (Fig. 9b). At  $t/t_f$  of about 0.87, where the water level stand right below the burrow, levee settlement increased and became slightly non-uniform with more settlement near the waterside (Fig. 9c). When the burrows became fully inundated ( $t/t_f \cong 0.97$ ), additional deformation was observed, and the cylindrical shape of the burrow experienced a substantial distortion, creating non-uniform diameter as illustrated in Fig. 9d.

4.2 Hydraulic performance and progressive failure

The pore pressure readings taken at the three PPT locations (1, 2, and 3) during the experiments allowed for close investigation of the hydraulic performance of the levee. It is imperative to note that the previously described settlement and the associated changes in levee geometry may result in slight changes in the elevations of the installed PPT. This could subsequently lead to some variation in pore pressure readings. In order to consider this settlement

effect, the total head ( $h_t$ ) has been modified based on the elevation of the PPT after settlement ( $z_{mod}$ ), rather than the raw pore pressure readings. The modified values are estimated as follows:

$$z_{mod} = z_o - \Delta z \tag{1}$$

$$h_t = z_{mod} + h_p \tag{2}$$

where  $z_o$  is initial height of the PPT above the datum (levee base);  $\Delta z$  is settlement at the PPT location (linearly interpolated); and  $h_p$  is the pressure head (obtained by dividing the pore pressure reading by the unit weight of water ( $\gamma_w$ )).

The hydraulic gradient near the exit points was calculated based on the modified head by dividing the difference in total head ( $h_t$ ) by the distance between the two PPTs. Figure 10 shows the changes in hydraulic gradient at the three preselected locations 1, 2, and 3 for both the intact and deteriorated levee. Based on this arbitrary definition, the hydraulic gradient is found to be notably higher for the deteriorated levee compared to the intact case. This was

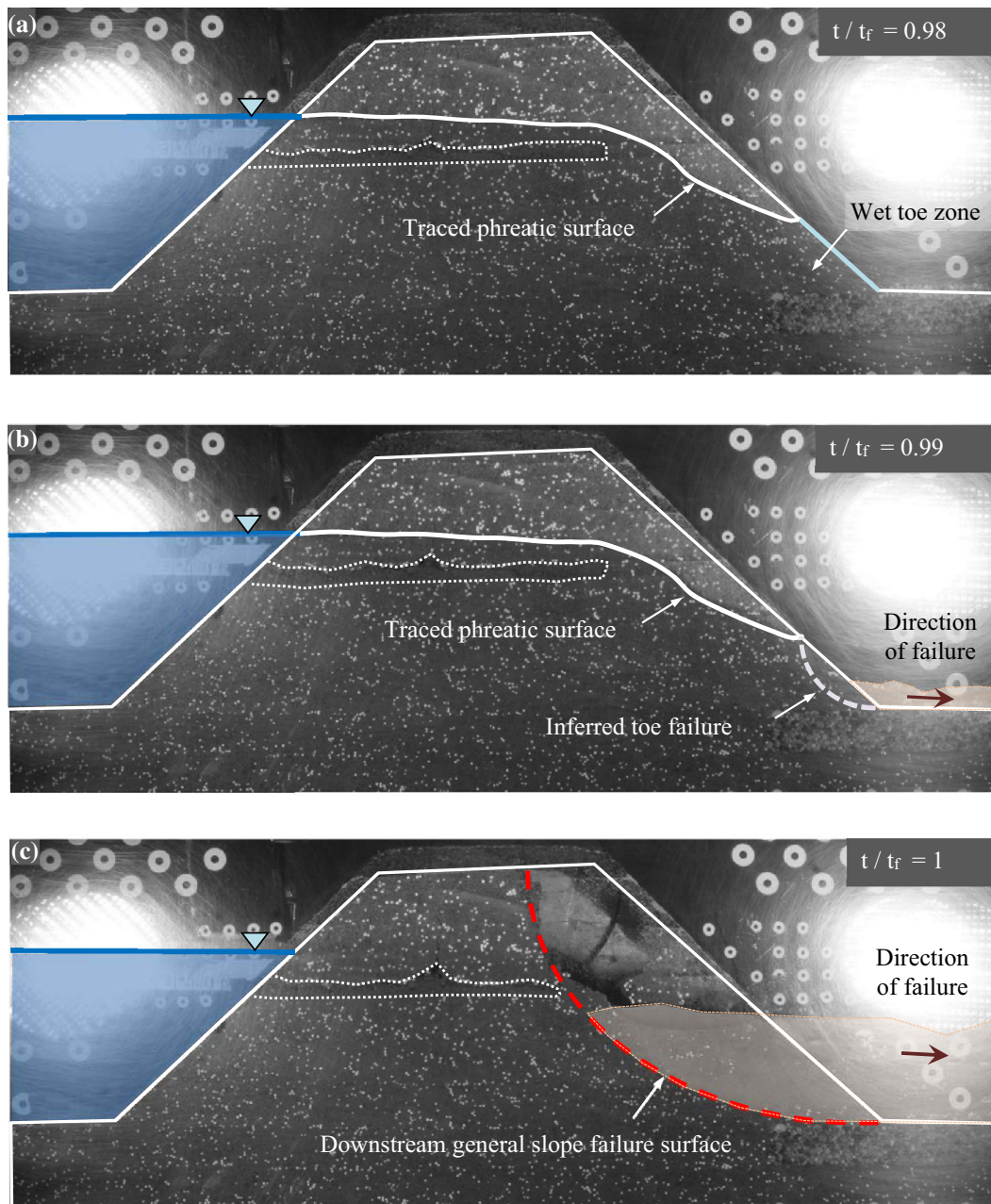


**Fig. 13** Progressive failure of levee with induced midnight burrows: **a** initially stable slope; **b** slope failure at the toe of the levee; **c** extension of the local toe failure to a global slope failure

globally observed with an increasing trend toward the exit slope in the vicinity of the toe drain.

The traced phreatic surfaces for the intact levee are depicted in Fig. 11 at the maximum retained water level. The phreatic surface appears to follow the theoretical pattern with an uninterrupted path ending at the toe drain. The slightly darker shades in Fig. 11 indicate the wet soil mass below the phreatic line. This is not, however, the case for the deteriorated levee as the presence of the water-filled

cavities appreciably altered the seepage path. The phreatic surfaces for both cases are conceptually illustrated in Fig. 12. For the deteriorated levee, the phreatic surface became essentially horizontal along the burrow length and intersected with the landside slope. In this case, the phreatic surface further advances horizontally leaving a larger wet area above the toe drain with the water flow exiting through the slope. Piping was observed during the experiment immediately before slope failure. Figure 13 shows

the local and global failure mechanisms developing in a deteriorated levee for  $t/t_f$  ranging from 0.98 to 1.0. The inferred phreatic surface is overlaid on the profile of the deteriorated levee as schematically shown in Fig. 13a. The noted changes to the default hydraulic response progressively lead to soil piping within the wet zone located above the toe drain, which results in local toe failure as shown in Fig. 13b ( $t/t_f \approx 0.99$ ). As illustrated in Fig. 13c, immediately following the toe failure and with further water seepage and soil erosion, a sudden global failure was developed ( $t/t_f \approx 1$ ). The near circular slope failure started from the levee crest and ended at the toe with a large soil mass moving along with the seeping water toward the landside.

## 5 Summary and conclusions

The hydraulic performance and failure mechanism of a deteriorated levee impacted by animal burrows have been experimentally investigated in this study. Centrifuge tests were conducted on instrumented intact and deteriorated levee models. Crest settlement as well as the changes in pore pressures were measured during the experiment. Idealized cylindrical burrows were created on the waterside of the levee and extended to about 75 % of the levee width (at the burrow location). Results confirmed that the presence of cylindrical cavities has a significant impact on the seepage pattern and as importantly on the overall stability of the levee. It has been demonstrated that cylindrical burrows can remain stable even when they are filled with water, and this alters the phreatic surface leading to an appreciable increase in hydraulic gradient above the levee toe. These changes were found to cause local slope failure at the toe of the slope. The progressive development of global failure was found to occur abruptly after the local failure resulting in water inundating landside. These findings could explain the unexpected and occasionally imminent failures of existing levees deteriorated by wildlife activities [2].

It should be noted that the complexity of real animal cavities do not warrant accurate duplication of burrow configuration that unarguably challenge any plausible optimization modeling scheme. Therefore, the results reported in this study reflect the behavior of the chosen levee geometry and soil type. Further investigation is, therefore, needed to study the response of earth structures with different side slopes and material types to other burrow configurations.

**Acknowledgments** This research is supported by the Natural Sciences and Engineering Research Council of Canada (NSERC) under Grant No. 311971-11. The assistance of the support staff at C-CORE centrifuge center is highly appreciated.

## References

- Adhikari S, Song CR, Cheng AH-D (2014) Evaluation of I-wall in New Orleans with back-calculated total stress soil parameters. *Acta Geotechnica* 9(6):1123–1134
- Bayoumi A, Meguid M (2011) Wildlife and safety of earthen structures: a review. *J Fail Anal Prev* 11(4):295–319
- Beek VMV, Knoeff JG, Rietdijk J, Sellmeijer JB, Cruz JLDL (2010) Influence of sand and scale on the piping process-experiments and multivariate analysis. Paper presented at the physical modelling in geotechnics, Switzerland
- Blach M, Jurist K, Morton S (2010) Anticipating California levee failure: government response strategies for protecting natural resources from freshwater oil spills. U.S. Department of the Interior Office of Environmental Policy and Compliance, Region IX
- Bonelli S, Brivois O (2008) The scaling law in the hole erosion test with a constant pressure drop. *Int J Numer Anal Methods Geomech* 32(13):1573–1595
- Boukhemacha MA, Ioan B, Khoudir M (2011) Theoretical mathematical modeling for piping erosion near conduits, vol 7. Technical University of Civil Engineering from Bucharest, Bucharest
- Camici S, Moramarco T, Brocca L, Melone F, Lapenna V, Perrone A, Loperte A (2010) On mechanisms triggering the levee failure along the Foenna stream on 1st January 2006 and which caused the flooding in the urban area of Sinalunga, Tuscany Region (Italy). A case study. *Geophys Res Abstr* 12:12037
- Chlaib HK, Mahdi H, Al-Shukri H, Su MM, Catakli A, Abd N (2014) Using ground penetrating radar in levee assessment to detect small scale animal burrows. *J Appl Geophys* 103:121–131
- Fell R, Wan CF, Cyganiewicz J, Foster M (2003) Time for development of internal erosion and piping in embankment dams. *J Geotech Geoenviron Eng* 129(4):307–314
- FEMA (2005) Technical manual for dam owners: impacts of animals on earthen dams
- Hansen DT (2008) Risk analysis, GIS and arc schematics: California Delta levees. Presented by David T. Hansen at the ESRI User Conference, San Diego California, 6 August 2008
- Hori T, Mohri Y, Kohgo Y, Matsushima K (2006) Model test and deformation analysis for failure of a Loose Sandy embankment dam by seepage. *Unsaturated Soils* 2:2359–2370 ASCE
- Hori T, Mohri Y, Kohgo Y, Matsushima K (2011) Model test and consolidation analysis of a Loose Sandy embankment dam during seepage. *Soils Found* 51(1):53–66
- International A (2007) Standard test method for particle-size analysis of soils, vol D. ASTM, USA
- International A (2009) Standard test methods for particle-size distribution (gradation) of soils using Sieve analysis. ASTM D6913, vol 4, ASTM, USA
- International A (2012) Standard test methods for laboratory compaction characteristics of soil using standard effort (12 400 lbf/ft<sup>3</sup> (600 kN-m/m<sup>3</sup>)), vol D. ASTM, USA
- Laundn JW, Reynolds TD (1993) Effects of soil structure on burrow characteristics of five small mammal species. *Great Basin Nat* 53(4):358–366
- Lominé F, Scholtès L, Sibille L, Poullain P (2013) Modeling of fluid–solid interaction in granular media with coupled lattice Boltzmann/discrete element methods: application to piping erosion. *Int J Numer Anal Methods Geomech* 37(6):577–596
- Mierzwa M, Suits B (2005) Jones tract, levee break DSM2 simulation. Methodology for flow and salinity estimates in the Sacramento-San Joaquin Delta and Suisun Marsh. 26th Annual Progress Report, <http://modeling.water.ca.gov/delta/reports/annrpt/2005/2005Ch3.pdf>

20. McCann MW (1999) plant and animal penetrations of dams incidents. ASSO/FEMA specialty workshop on plant and animal penetrations of earthfilled dams on USDA forest service dams, 30 Nov–3 Dec 1999, University of Tennessee Conference Center, Knoxville, TN
21. Ohio Emergency Management Agency. [http://ema.ohio.gov/Documents/OhioMitigationPlan/SOHMP\\_Sec\\_2\\_6.pdf](http://ema.ohio.gov/Documents/OhioMitigationPlan/SOHMP_Sec_2_6.pdf). Accessed 23 August 2010
22. Rocscience Inc. (2003) Slide v5.0—two-dimensional limit-equilibrium analysis of soil and rock slopes. Verification Manual Part I
23. Schmocker L, Hager WH (2012) Plane dike-breach due to overtopping: effects of sediment, dike height and discharge. *J Hydraul Res* 50(6):576–586
24. Sellmeijer H, de la Cruz JL, van Beek VM, Knoeff H (2011) Fine-tuning of the backward erosion piping model through small-scale, medium-scale and IJkdijk experiments. *Eur J Environ Civil Eng* 15(8):1139–1154
25. Sharp JA, McAnally WH (2012) Numerical modeling of surge overtopping of a levee. *Appl Math Model* 36(4):1359–1370
26. Sills G, Vroman N, Wahl R, Schwanz N (2008) Overview of New Orleans levee failures: lessons learned and their impact on national levee design and assessment. *J Geotech Geoenviron Eng* 134(5):556–565
27. Slogar B (1999) Animal penetrations into earthen embankments. ASSO/FEMA specialty workshop on “Plant and Animal Penetrations of Earthfilled Dams”, pp 189–193, 30 Nov–2 Dec 1999, University of Tennessee Conference Center, Knoxville, TN
28. van Beek VM, Knoeff H, Sellmeijer H (2011) Observations on the process of backward erosion piping in small-, medium- and full-scale experiments. *Eur J Environ Civil Eng* 15(8):1115–1137
29. Washington Dept. of Ecology, [www.ecy.wa.gov/programs/wr/dams/Reports/damfailure\\_ws.pdf](http://www.ecy.wa.gov/programs/wr/dams/Reports/damfailure_ws.pdf). Accessed 13 Sept 2010
30. Washington Dept. of Ecology. <http://www.ecy.wa.gov/programs/wr/dams/iowa.html>. Accessed 21 Sept 2010
31. X-J Zhou, Y-X Jie, G-X Li (2012) Numerical simulation of the developing course of piping. *Comput Geotech* 44:104–108